A Model for Current-Voltage Oscillations at the Silicon Electrode and Comparison with Experimental Results

Journal of The Electrochemical Society, **146** (3) 1134-1140 (1999)
S0013-4651(98)05-017-4 CCC: $7.00

A Model for Current-Voltage Oscillations at the Silicon Electrode and Comparison with Experimental Results

J. Carstensen, R. Prange,* and H. Föll**

Faculty of Engineering, Christian-Albrechts-Universität zu Kiel, 24143 Kiel, Germany

The first consistent and complete model of current oscillations at the Si electrode is presented. The only basic assumption needed is an ionic breakthrough mechanism which is postulated to occur in thin oxides under oxidizing electrode conditions, leading to an enhanced and localized ion transport to the Si-SiO_2 interface. Choosing reasonable values for three corresponding physical parameters and using a Monte Carlo simulation technique, first-principle calculations yield quantitative data in excellent agreement with numerous experimental results, including the value of the current, surface roughness, the average oxide thickness, and the capacitance as a function of the phase of oscillations, and the frequency of the oscillations as a function of applied voltage, current density, etching rate or HF concentration, and temperature.

Manuscript submitted May 7, 1998; revised manuscript received September 4, 1998.

The reactive solid-liquid contact is not too well understood in general, and this is particularly true for the Si-liquid contact. Even the supposedly simple chemical etching of Si or SiO_2 is still full of surprises, as anyone employed in microelectronics will acknowledge. More specifically, a case could be made that the current-carrying solid-liquid contact with Si as the electrode and an electrolyte containing some F^- ions, commonly in the form of diluted HF, is not understood at all. Nobody can predict the complex features of the current-carrying Si-HF contact. Not even the voltage-current characteristics obtained in simple experiments are computable from first principles. Porous silicon, with an increasing wealth of features that are mostly not understood,[1,2] and the totally mystifying current-voltage oscillations that occur in a large region of the available parameter space,[2-4] bear witness to this claim.

This paper deals exclusively with voltage-current oscillations in Si, but it is worthwhile to point out that this phenomenon is not specific to the Si electrode. In fact, it was Faraday some 100 years ago who remarked on oscillating electrodes (a term we use for both current or voltage oscillations, depending on the experimental conditions chosen),[5] but until now no general model has been developed. The recent interest in Si electrochemistry, triggered by the observation that one kind of porous Si shows strong luminescence,[6,7] has also spurred a number of investigations into the current-voltage oscillations observed under special but easily established conditions in Si.[8-14] It is now generally accepted that oscillations can occur under conditions where an oxide is formed by the current and is in turn dissolved by the electrolyte. However, despite these recent efforts, not one single consistent model of electrode oscillations has been suggested so far.[15]

Any model of an oscillating electrode needs three ingredients: First, a mechanism for a local oscillator is required. This is obvious, because without an atomic-scale oscillation mechanism, no oscillations can occur. More specifically, a mechanism that describes some nonlinear behavior of the electrode on an atomic scale must exist, because linear relations, e.g., the linear interplay of oxide formation proportional to the current and chemical oxide dissolution, does not lead to stable oscillations but to a steady-state equilibrium, as already pointed out by Franck in 1978.[16]

Still obvious, after some deliberation, is the second ingredient. A synchronization mechanism that forces at least some of the local oscillators to synchronize is a must for "macroscopic" electrode oscillations, i.e., oscillations observed with specimens of macroscopic dimensions. Local current oscillators that are not synchronized to some extent will, if summed up to yield the total current, lead to an average current that shows no oscillation but at best some "colored" noise.

Less obvious is the third and last ingredient needed for any complete model of an oscillating electrode. Perhaps surprisingly, a desynchronization mechanism is needed just as well. This is so because otherwise electrodes would either oscillate strongly or not at all. Many phenomena that are observed (e.g., damped oscillations[17]) or predicted (nonsynchronized oscillations that manifest themselves in "colored" noise), would be impossible without a mechanism that opposes synchronization.

In this paper a complete model of the oscillating Si electrode under "low-frequency" conditions is presented for the first time. "Low-frequency" conditions, in a preliminary imprecise definition, are obtained for relatively low HF concentrations, voltages, or currents, respectively. The term is precisely defined in what follows, but it is prudent to point out at this stage that the model presented does not yet include all kinds of observed electrode oscillations.

Figure 1 illustrates a few of the experimental data that need to be modeled. The current density, $J(t)$ as a function of time, t, the frequency, $f(U_{an}, J, C_{HF})$, of the oscillations as a function of the applied anodic voltage, U_{an}, the current density, J, or the concentration of the electrolyte, C_{HF}, needs to be calculated, but also less obvious parameters such as the average oxide thickness, the capacitance of the solid-liquid junction, or the roughness of the solid surface, should be obtained with a complete model.

Model

We start with the generally accepted fact that the local mechanism of an oscillating Si electrode relies on the formation and dissolution of SiO_2. Several experiments demonstrate that the resulting oxide layer is less than 10 nm thick on an area and time average (see, e.g., Ref. 18 and 19).

On this base we first postulate that all the current flowing across the interface produces oxide at all times and in all places. This is the quantitative definition of the "low-frequency" condition; it must not be true for all oscillations observed. It is possible, e.g., at higher currents and frequencies, that some part of the current does not produce oxide, but this does not concern us in this paper. This is not a strong assumption and it poses no limits on the spatial or time dependence of the current. Local current flow thus always increases the local thickness, s, of the oxide layer. The oxide thickness in turn may still depend on position as well as on time: $s = s(x, y, t)$. The relation

$$\frac{ds(x, y, t)}{dt} = \beta J_{ox}(x, y, t) - \alpha(x, y, t) \qquad [1]$$

with β being a geometrically determined parameter (essentially the valence of the process, i.e., the number of holes needed to produce one SiO_2 unit) and α the purely chemically determined dissolution rate, must hold locally and at all times. The dissolution rate, to be totally general, must not be a constant but could depend on local con-

* Electrochemical Society Student Member.
** Electrochemical Society Active Member.

S0013-4651(98)05-017-4 CCC: $7.00 © The Electrochemical Society, Inc.

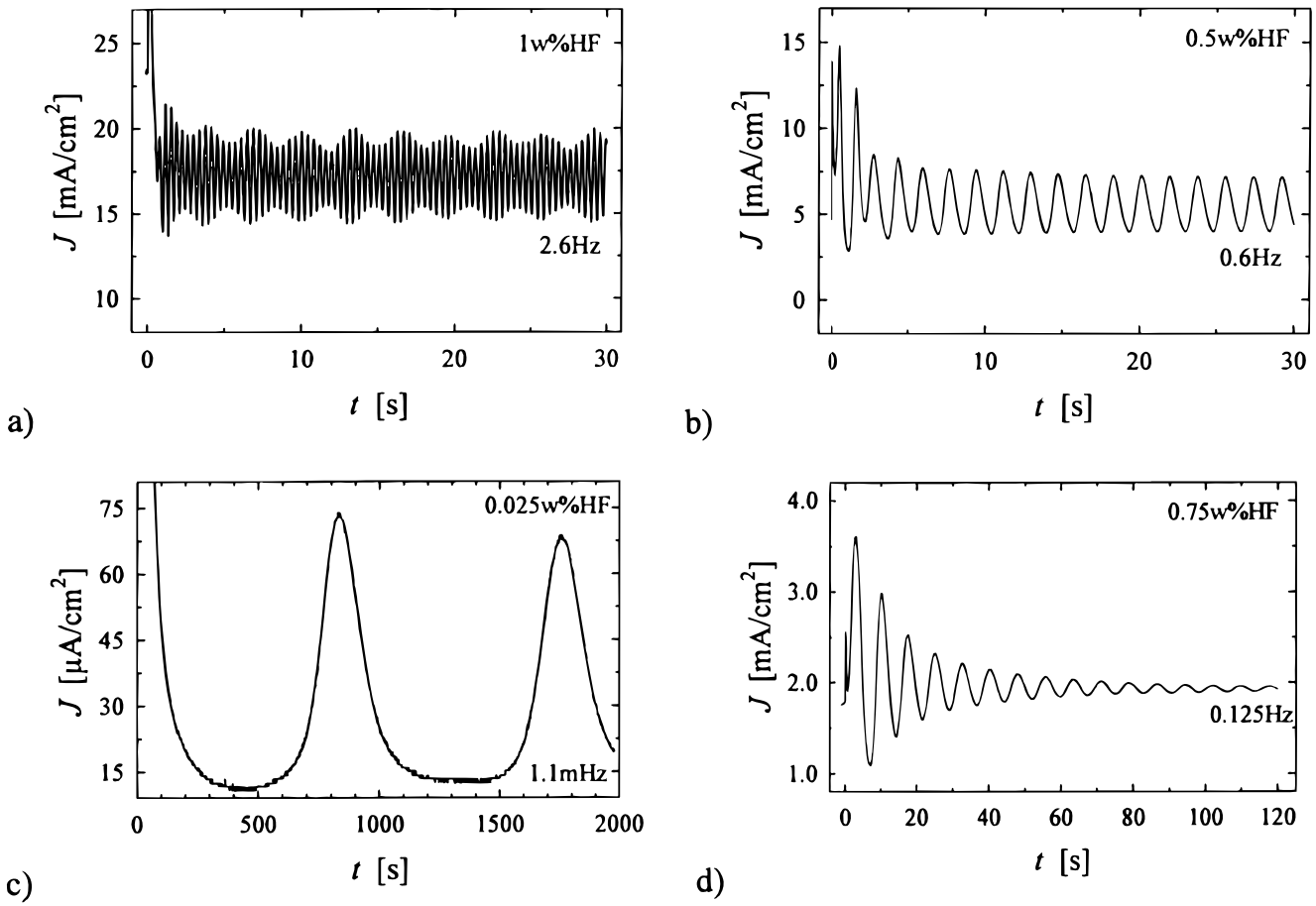

Figure 1. A set of current vs. time measurements shows different features of the oscillating Si-HF-system. (a-c) Applying a constant anodic potential $U_{an} = 5$ V, the frequency and shape of the oscillation differ strongly. (a) Almost chaotic behavior, (b) sine waves, and (c) very asymmetric oscillation are observed. Upon reducing the potential to $U_{an} = 3$ V, (d) damped oscillations occur.

ditions. This would be the case, e.g., if the chemical dissolution rate depends on the field strength and therefore on the local thickness of the oxide, but also if the surface of the oxide is rough in some places but not in others. O^- ions must migrate through the existing oxide layer to be consumed at the interface. As already stressed by several authors,[4,20] the ion transport through the oxide layer holds the key for the understanding of the oscillation phenomenon. We propose in our only strong assumption that the strong electric field present across the (thin) oxide is a nonlinear driving force for the ion transport through the oxide. Since a uniform field-enhanced diffusion is not sufficiently nonlinear, we propose an "ionic breakthrough" mechanism. Whenever the electric field in the oxide approaches an upper critical value, E_{max}, a breakthrough channel or pore is formed, leading to a highly localized ionic current, J_{ox}, to be matched by the hole current at the interface that is largely independent of oxide thickness. At and around the pore tip the oxidation is enhanced, leading to a roughly semispherical oxide "inclusion" around the pore. Since SiO_2 formed from a given volume of Si almost doubles in volume, a corresponding bump is formed on the oxide-electrolyte interface, i.e., the oxide surface. Figure 2a illustrates this mechanism. Inherent in this mechanism is a lateral growth of oxide relative to the pore tip, resulting from rapid diffusion of O^- ions in the SiO_2-Si interface or from a movement of the channel end to the thin part of the oxide.

It is unimportant for the model exactly how the ionic breakthrough occurs or which mechanism establishes lateral oxide growth in which precise geometry. It is likely that the ionic breakthrough is linked to or even triggered by a normal (avalanche) electronic breakthrough, but since this is of no importance for what follows, we do not discuss or speculate about the detailed mechanisms.

We now specify our basic assumption in order to enable quantitative modeling. While the oxide thickness increases around the pore tip, the electric field decreases without reducing the ion transport through the oxide. At a minimum value, E_{min}, the oxide growth stops. This means that in analogy to an electronic breakthrough, we postulate that after starting the ion transport through the oxide, the electric field can be reduced significantly without reducing the ion current. Leaving aside a microscopic picture for the ion transport and only pointing out that the ions have to pass a 2-8 nm thick oxide layer, a mechanism emerges centering around a narrow (1 nm or less) channel or pore through the oxide which is opened at high field strength and closed at low field strength. With the local anodic potential, U_{an}, and defining E_{max} as the maximal field strength needed for ionic breakthrough and E_{min} as the minimal field strength for the ending of the ionic current flow, the relations

$$s_{min} = \frac{U_{an}}{E_{max}} \quad \text{and} \quad s_{max} = \frac{U_{an}}{E_{min}} \qquad [2]$$

for the minimum and maximum oxide thickness, s, are obtained. The local oxide layer thickness thus increases by approximately

$$\Delta s = s_{max} - s_{min} \qquad [3]$$

while the channel is "open."

This model reverses ideas previously presented[2] where an electronic breakthrough leading to a locally enhanced nonoxidizing current was envisioned as the cause for electrode oscillations. It is obvious that the ionic breakthrough mechanism indeed provides for the required local oscillator. However, as stated previously, it does not

S0013-4651(98)05-017-4 CCC: $7.00

necessarily account for macroscopic oscillations that can only be observed when a large number of local oscillators are synchronized. This is true even for the case of a perfectly homogeneous electrode where all local oscillators would start at the same time, because we have to make allowances for the statistical nature of the postulated breakthrough process. E_{min} and E_{max} must be seen as lower and upper limits for the ionic breakthrough (or "opening" and "closing") of the channels, and in accounting for the statistical nature of these events, we have to define two functions, $W(E)$ and $R(E)$, which give the probability for the opening and the closing of a channel within a time Δt on an area ΔA. These functions are detailed in the Appendix.

The statistical nature of the proposed process, aside from the more realistic situation where the oxide layer would never be totally homogeneous over large areas at any one time during an oscillation, would necessarily cause a rapid desynchronization of originally synchronized local oscillators. No macroscopic oscillations would be observed after some time, because the local currents are then summed up with random phases, yielding a constant, if noisy, macroscopic current. We emphasize that a nonoscillating electrode in this model does not prove the absence of local oscillations but may only show the absence of a synchronization mechanism. If one were to measure the spectral intensity of the current noise, we predict that in this case a strong peak would be present at the typical frequency of the local oscillators.

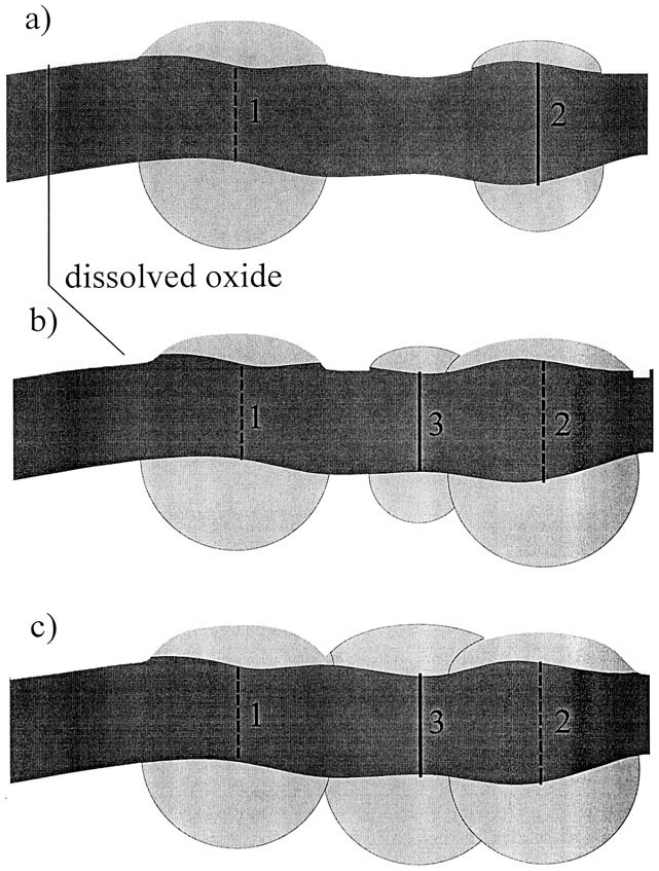

Figure 2. A highly schematic view of the oxide growth mechanism. (a) Channel 1 is already closed while channel 2 is open. Both pores are growing independently because they do not overlap. (b) A third channel opens between channel 1 and 2 if the desynchronization is small, i.e., the anodic potential at channel 3 is not too much decreased by the current through channel 2. (c) The closing of channel 3 is early and thus synchronized to channel 1 and 2, because channel 3 needs to grow less oxide for the "closing" to take place. This mechanism leads to a nearly homogeneous growth of the oxide layer. The chemical dissolution occuring all the time (shown, roughly to scale, by the lightly shaded areas) smoothes the surface even more.

Our local oscillator, however, has a built-in synchronization mechanism with respect to its nearest neighbors. This results from the lateral growth of the oxide around the pore tip as illustrated in Fig. 2a-c. Let us assume that a new channel (no. 3 in Fig. 2b) is opened close to an active one (no. 2 in Fig. 2b). This neighboring channel then must produce less oxide before it stops again, because it is "helped" by the already active pore (cf. Fig. 2c). Its stopping point is thus already much closer to the stopping point of the first channel; we could say that its dynamics are enhanced until it catches up with the first oscillator. After a few cycles (in fact one is sufficient) the two local oscillators are well synchronized.

A desynchronization mechanism, as previously pointed out, is also needed for a realistic model. It too, exists as an intrinsic property of the local oscillator model. Once a channel opens, the current density is locally increased, leading to increased ohmic and diffusion losses which locally reduces the potential across the oxide layer (see Fig. 3a). This reduces the electric field strength in the neighborhood of an active channel and therefore the probability for a breakthrough next to an active pore.

Applied to the example given, this effect would slow down the dynamics of the oscillator until it is perfectly out of phase. Consequently not all areas of the oxide layer could grow at the same time, which indicates a desynchronization of the macroscopic oscillation. Assuming a reduction of the current density $J(r) \propto r^{-2}$ at a distance r from the channel, the electric field shows the cylindrical geometry of Fig. 3b and the losses for the applied potential are given in a first approximation by

$$\Delta U_{an}(r) = -\frac{A}{r} \qquad [4]$$

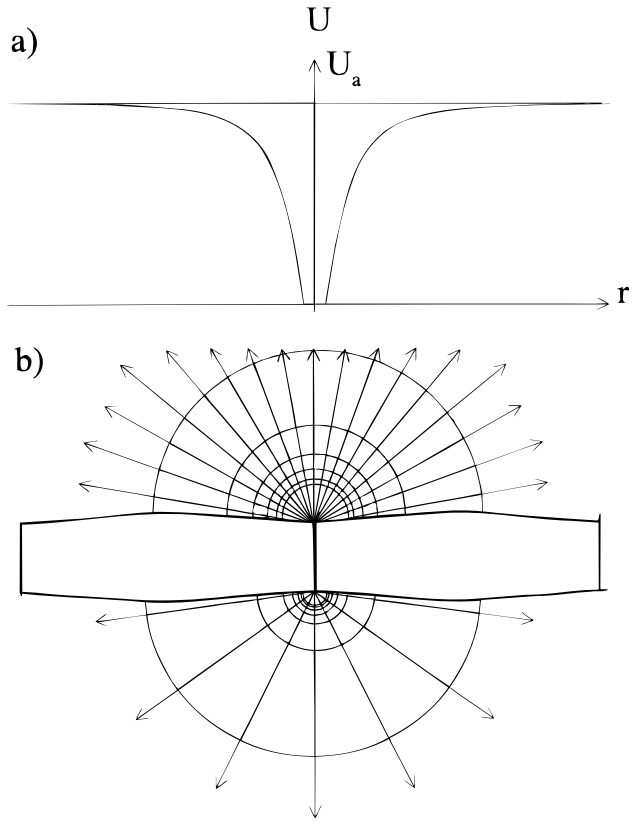

Figure 3. The decrease or lost $\Delta U_{an}(r)$ of the anodic potential due to high local current densities are plotted in (a) as a function of the distance r from a breakthrough channel. (b) The corresponding current field and equipotential lines needed to obtain a field strength that decreases by $\approx r^2$ on both ends of the channel. The schematic drawing is roughly to scale relative to the oxide thickness.

S0013-4651(98)05-017-4 CCC: $7.00

As a first approximation this function is used to describe the potential and diffusion losses of the anodic potential in the Monte Carlo simulations with A as a fitting parameter.

We now show that the model described can account for most, if not all observations in the low-frequency domain.

Analytical Results

To summarize, our model contains (*i*) local oscillators caused by oxide growth in an ionic breakthrough mechanism; (*ii*) synchronization of local oscillators by nearest-neighbor interaction due to lateral growth at the breakthrough channel tips; and (*iii*) desynchronization by ohmic or diffusion losses of the anodic potential at local oscillators. The performance of the model and its dependence on parameters is analyzed by Monte Carlo simulations, but before discussing these general results, some qualitative features and analytical formulas for the case of well-synchronized oscillations are presented.

One important feature of the model is that it provides for a persistent, but changing roughness of the oxide surface as well as the Si-oxide interface. The local oscillators, if active, always produce rather pronounced bumps during the oxide-building phase, as shown in Fig. 2. The chemical dissolution of the oxide, however, tends to smooth the surface and thus reduces the roughness. This is an important feature with repercussions to the calculation of, e.g., capacitance or dielectric constants as obtained by averaging measurements such as ellipsiometry.[8] The Monte Carlo simulations provide a detailed and quantitative picture of this process; here we just keep in mind that the speed of a chemical dissolution process depends on surface roughness since it is roughly proportional to the surface area.

For very slow oscillations the time for building up the oxide can be neglected compared to the time for dissolving the oxide. This can be seen directly in the current-voltage curves of Fig. 1, where a short current peak corresponding to oxide growth is followed by a long period of low current corresponding to oxide dissolution. The time, T, for one oscillation period is therefore approximately $T = \Delta s/\alpha$. Using the electric field–defined dynamics for the local oscillators as discussed previously, we find

$$T = \frac{\Delta s}{\alpha} = \frac{s_{\max} - s_{\min}}{\alpha} = \frac{U_{\text{an}}}{\alpha}\left(\frac{1}{E_{\min}} - \frac{1}{E_{\max}}\right) \qquad [5]$$

This linear correlation between T and U_{an} is by no means obvious, because for high-frequency oscillations, which are not included in this model, the reverse is true, i.e., the oscillation time decreases with increasing potential.[21] For extremely diluted HF electrolytes and thus a slow dissolution rate α, the oscillation time then increases linearly as a function of the applied voltage, as experimentally shown in Ref. 4 and 22 or in our own measurements (Fig. 4). In addition, the frequency $f = 1/T$ should be proportional to α; but this is much more difficult to ascertain experimentally, because changing the HF concentration and therefore α, also changes other properties of the Si-HF contact. Nevertheless, a linear correlation between the frequency and the dissolution rate was found experimentally in Ref. 12. Note that α is the only strongly temperature-dependent parameter in Eq. 4. This allows for appropriate experiments as a test of the model. As a last remark, α must not be taken as the dissolution rate of normal oxide in HF. Due to the persistently rough nature of the oxide surface, the dissolution rate on the average is enhanced by a factor of approximately 1.7, as shown in Ref. 14. For stable oscillations the mean oxide layer thickness does not change, i.e., applying Eq. 1 we find

$$0 = \overline{\frac{ds(x, y, t)}{dt}} = \beta\overline{J_{\text{ox}}(x, y, t)} - \alpha \qquad [6]$$

The bar denotes the averaging across the complete electrode area and over one oscillation period. The mean oxidizing current thus is

$$\bar{J}_{\text{ox}} = \frac{\alpha}{\beta}, \quad \text{or} \quad \alpha = \beta\bar{J}_{\text{ox}} \qquad [7]$$

Inserting Eq. 6 in Eq. 4 we find

$$f = \frac{1}{T} = \frac{\beta}{U_{\text{an}}}\left(\frac{1}{E_{\min}} - \frac{1}{E_{\max}}\right)^{-1}\bar{J}_{\text{ox}} \qquad [8]$$

This correlation between oscillation frequency and mean current density has experimentally been shown in Ref. 14 and 22.

The model thus allows generation of the correct relations of observable parameters and agrees qualitatively with experimental results. In the remainder we demonstrate that with a reasonable set of model parameters the equations given supply quantitative data which match perfectly all experimental data known to us.

Results from Monte Carlo Simulations

Implementing the model.—Monte Carlo simulations are implemented on a PC and were performed for various sets of model parameters as discussed in the Appendix. The quantitative results depend on the parameters used to implement the model. The case of extremely diluted hydrofluoric acid with a dissolution rate of α = 0.04 nm/s was chosen, which was calculated from our own experimental data using an electrolyte concentration of 0.05 wt % HF in Ref. 14. There are also independent data for α [23] that give values very close to the chosen one; α thus can be considered to be a known parameter for the model.

An assumption has to be made for the critical electric field strengths. We chose $E_{\min} = 5 \times 10^6$ V/cm and $E_{\max} = 3 \times 10^7$ V/cm, which not only suits experimental results relating to current transient measurements described in Ref. 14, but is compatible with the electronic breakthrough strengths of thin oxides.[24] Again, admittedly with some more uncertainties as in the case of α, the critical field strengths are in essence known parameters of the model.

We further assume a constant oxidizing current of 0.1 fA through each open channel as discussed in the Appendix. This value is determined by the average current density and the geometry of the process and can also be viewed as a known parameter and not a fit parameter of the model.

More critical is the choice of some appropriate probability functions $W(E)$ and $R(E)$, since not much is known about these functions from independent experiments. It is, however, very likely that oxides with rather large breakthrough field strengths will not have very "soft" probability functions. Bearing this in mind, we fitted reasonable functions so as to obtain best results. (See the Appendix for details.)

For the desynchronization as described by Eq. 4, we take A = 0.2 V nm. This is the only parameter in the model that is mostly determined by fitting, because no independent estimate could be made so

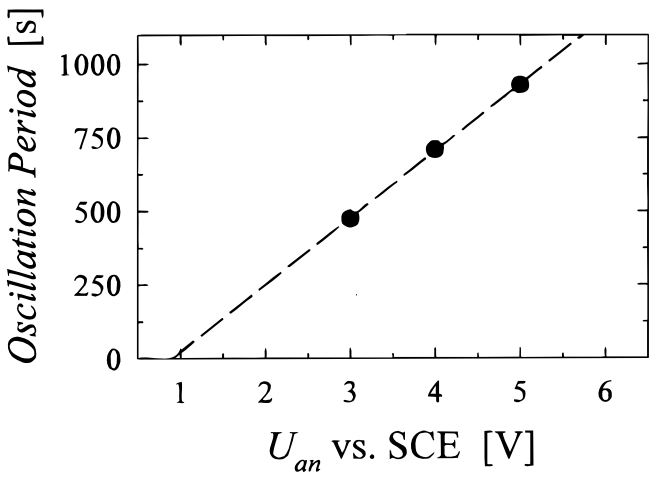

Figure 4. For extremely slow current oscillations, the oscillation period is measured as a function of applied anodic potential. We find a straight line in agreement with Eq. 5.

S0013-4651(98)05-017-4 CCC: $7.00

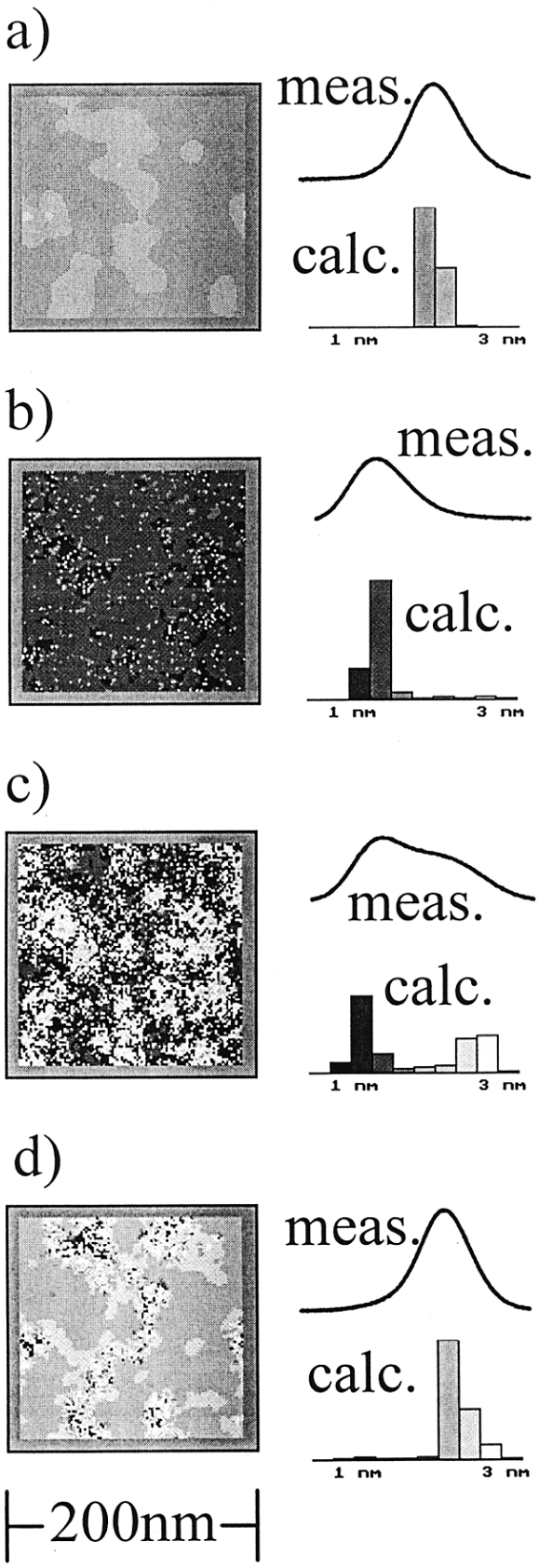

Figure 5. A series of "snapshots" of the oxide layer thickness obtained by Monte Carlo simulations demonstrates the strong coupling due to percolation of the oxide layer thickness. The calculated histograms are compared with the measured distribution functions of the oxide layer thickness reported in Ref. 12.

far. Figure 3 shows, roughly to scale, the physical implications of the chosen value. Stable macroscopic oscillations, damped oscillations, unsynchronized oscillations, or no oscillations at all can be obtained by varying *A*. We return to this parameter in the Discussion.

In essence, the model needs three parameters that have to be obtained primarily by fitting model data to experiments.

Results

Figure 5a-d shows maps of the oxide layer thickness on an 200 × 200 nm area for subsequent phases of one oscillation period. Most important is the lateral coupling of local oscillators in areas more than 100 nm in size, although there is no mechanism implemented in the model to force such large areas to nearly the same thickness. What happens is that the lateral synchronization of these areas is caused by percolation due to the local coupling mechanism, which consequently leads to synchronization in the time domain and to macroscopic oscillation. If the anodic potential is reduced, or the parameter *A* in Eq. 4 (and thus desynchronization) is increased, no macroscopic current oscillations manifest the still-existing local oscillations. The corresponding oxide thickness map $s(x, y)$ of Fig. 6 shows a random distribution for $s(x, y)$, and the histogram in Fig. 6 may be interpreted as the average of the histograms in the oscillating case of Fig. 5.

The calculated data of the Monte Carlo simulation can be compared with experimental results. First, the thickness distribution of the oxide layer, e.g., the oxide layer distribution function $D(s)$, which determines the total area of the oxide with thickness s, can be directly obtained. Comparing our calculated histograms in Fig. 5a-d with the experimentally determined distribution function given in Ref. 14, we find an almost perfect agreement for all phases of the oscillation. It should be emphasized that the calculated and the measured distribution function would be completely independent if only their shape is compared; the agreement of the numerical values, however, is to some extent the result of the fitting of the three parameters mentioned to the absolute thickness values of the oxide, as given in Ref. 14.

If the same set of parameters employed in the Monte Carlo simulations is used for Eq. 5, we can calculate, e.g., the frequency of the oscillations as a function of the applied voltage and compare the results with experiments in Fig. 4. The agreement is perfect, providing an independent proof of the validity of our assumptions. Similar results are obtained for the frequency-current relations.[22]

Going beyond the analytical formulas and using the distribution function $D(s)$ obtained from the histograms, we can now calculate a number of measurable quantities, e.g., the mean oxide thickness

$$\langle s \rangle = \int sD(s)ds \qquad [9]$$

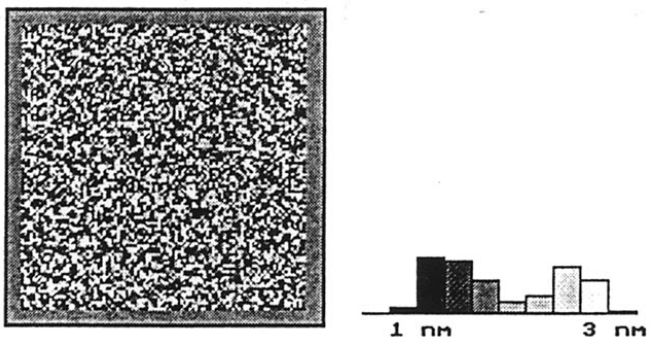

Figure 6. The map of the oxide layer thickness for a nonoscillating macroscopic current shows no percolation areas. The distribution function of the oxide layer thickness may be interpreted as the average of the distribution functions of a macroscopically oscillating system.

S0013-4651(98)05-017-4 CCC: $7.00

the oxide roughness

$$R = \int |s - \langle s\rangle| D(s) ds \qquad [10]$$

capacitance

$$C = \epsilon\epsilon_0 \int \frac{1}{s} D(s) ds = \epsilon\epsilon_0 \left\langle \frac{1}{s} \right\rangle \qquad [11]$$

and the ratio

$$\epsilon_{\text{virtual}} = \langle s\rangle \left\langle \frac{1}{s} \right\rangle \qquad [12]$$

which is the "virtual" change needed for the dielectric constant ϵ of SiO_2 if the capacitance is calculated from the mean oxide thickness according to $C = \epsilon\epsilon_{\text{virtual}}\epsilon_0(1/\langle s\rangle)$.

One set of results is shown in Fig. 7A-E. In order to demonstrate the strong synchronization due to nearest-neighbor interaction and percolation, we chose random starting conditions, i.e., a random distribution of oxide thickness, but this generates only small aberrations in the first period of oscillations.

The current oscillations obtained from the calculation perfectly match the shape of the experimental curve given in Fig. 1c. To better understand the oscillation process, four points in Fig. 7A, corresponding to specific changes in the oscillation process, are labeled a-d and are discussed. The computed images in Fig. 5a-d correspond exactly to the marked points in Fig. 7A; an interpretation of the particular state of the electrode at the four points is thus possible.

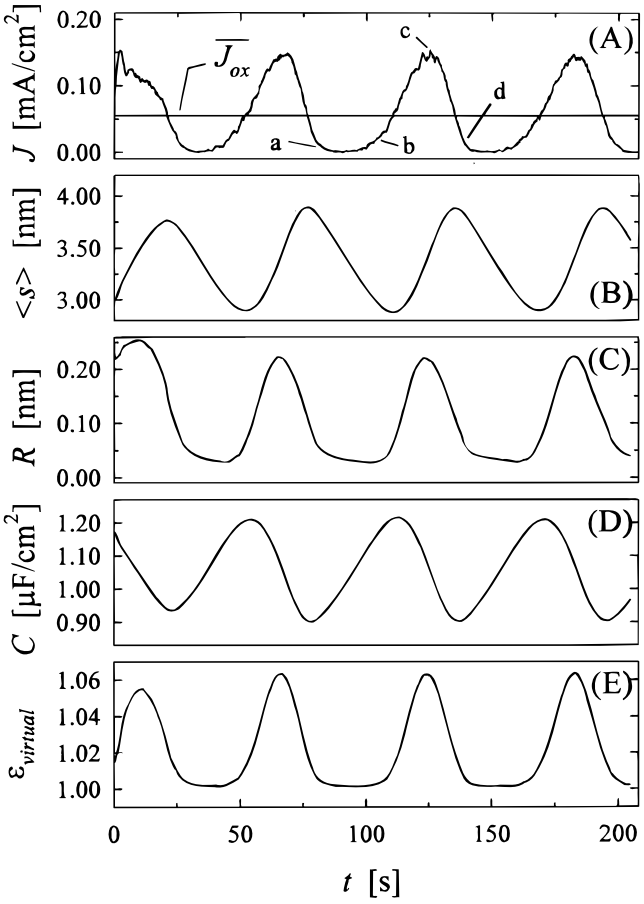

Figure 7. As a result of the Monte Carlo simulation, current (*A*), mean oxide thickness (B), surface roughness (C), capacitance of the oxide layer (D), and the relative change in the dielectric constant $\epsilon_{\text{virtual}}$ are plotted as a function of time. In (A) distinct times of the oscillation are marked corresponding to the maps in Figure 5a-d. The average oxidation current density, J_{ox} equals the current density, *J*, whenever its capacitance, C_{ox}, is maximal or minimal.

At point a we find a nearly homogeneous thick oxide layer, which is dissolved with a nearly constant rate α up to about point b, where first oxide areas show ionic conductivity and are growing quickly while most of the oxide is still thinning. Point c marks the phase of the oscillation with maximum oxide current. At this point, about half of the area of the oxide is still only dissolving while on the other half the oxide has already reached its maximum thickness. In point d the cycle is almost closed. Most areas show thick oxide layers and are only chemically dissolved, while some remaining areas with thin oxide suffer ionic breakthrough and increase their thickness. Consequently, whereas the synchronization process is strong enough to produce macroscopic current oscillations, the electrode is far from behaving in a homogeneous manner.

Next we discuss Fig. 7B, showing the mean thickness of the oxide. As expected, it decreases linearly between a and b, because only chemical etching takes place. The maxima and minima necessarily cannot coincide with the current extrema but can be easily calculated. Since they correspond to $ds/dt = 0$, we find their location at the intersection of the current curve with the mean current J_{ox} given in Eq. 7. The intersection points are shown in Fig. 7A.

A remarkable feature of the model is its ability to provide data about the surface roughness, Fig. 7C shows that the roughness, as defined in Eq. 10, oscillates with a rather large amplitude and almost in phase with the current. If measured with an instrument that is not sensitive on a small scale (nanometers), but perceives only wavelengths in the 10 nm region, a waviness that roughly corresponds to the visual impression of Fig. 5a-d would be detected. A constant changeover between a relatively rough surface thus should be observed and was indeed observed by in situ atomic force microscopy (AFM) analysis in Ref. 19.

Next we calculate the capacitance of the system. Figure 7D shows the result and, as expected, shows that the capacitance increases roughly inversely proportional to the mean oxide thickness. If one just uses the mean oxide thickness, however, to compute the capacitance, the result does not fully agree with the measurements and it must be assumed that the dielectric constant also oscillates. This is so because the total capacitance of parallel capacitors differing in their oxide thickness is not determined by 1/<s> but rather by <1/s>. With the help of the equation

$$C = \epsilon\epsilon_0 \left\langle \frac{1}{s} \right\rangle = \epsilon\epsilon_{\text{virtual}}\epsilon_0 = \frac{1}{\langle s\rangle} \qquad [13]$$

it is possible to calculate the changes in ϵ that seem to be present (or that are directly measured with an ellipsometer if the raw data are processed on the basis of the mean oxide thickness) in measurements reported in Ref. 22.

Figure 7E shows $\epsilon_{\text{virtual}}$. The change of 5% seems to be negligible, but since the variation is given by

$$\left\langle \frac{1}{s} \right\rangle = \left\langle \frac{1}{s} \right\rangle^2 \delta\langle s\rangle \qquad [14]$$

the discrepancy increases strongly for thinner oxide layers obtained, e.g., at the higher frequencies employed in Ref. 22. In essence, we claim that ϵ is constant and does not change during an oscillation. Changes observed or computed are due to an averaging procedure that must not be applied for the rough oxides present during oscillations.

Discussion

First, we discuss a possible generalization of the model. Macroscopic oscillations result from the interplay of synchronizing and desynchronizing nearest-neighbor interactions and a percolation process which may spread synchronization over a large area.

Using Fig. 2 we can define a minimum distance *d* of two channels which can exist at the same moment. The critical field strength E_{max} has to be reached at *d*, which depends on the actual thickness, the applied potential, the probability function $W(E)$ and the ohmic

S0013-4651(98)05-017-4 CCC: $7.00

losses $\Delta U_{an}(r)$. If d is large and no third channel can open before one of the two existing channels is closed, the oxide cannot grow homogeneously and is rather rough. In contrast, if d is small, the oxide layer can grow nearly homogeneously, because the semispherical oxide inclusions overlap. It might be useful to find a geometric parameter $\xi(d,U_{an})$ which determines the ratio between the strength of the synchronization and the desynchronization mechanisms. Tentatively, we define

$$\xi = \frac{\Delta s}{d} = \frac{U_{an}}{d(U_{an})}\left(\frac{1}{E_{min}} - \frac{1}{E_{max}}\right) \qquad [15]$$

Beyond a critical value ξ_{crit} (yet to be determined), we expect macroscopic oscillations; otherwise, only colored noise is present. This analytical equation, if justified and worked out, could allow a simple and general calculation of whether macroscopic oscillations are to be expected, without resorting to Monte Carlo simulation. It may then be used to obtain phase diagrams of oscillating electrode systems.

Next, we critically review the fundamental assumptions of the model. Most basic is the ionic breakthrough hypothesis with the concomitant rapid oxide growth around the pore tip. No direct confirmation of this mechanism is known to us; it thus must be taken as an essential prediction of the model, verifiable, e.g., with high-resolution electron microscopy or scanning tunnel microscopy. It was already mentioned that the postulated ionic breakthrough may be inextricably linked with electronic breakthrough; here we point out that this may be the clue to the understanding of high-frequency oscillations which are not included in this model.

The parameters coupled to the ionic breakthrough are less critical. The exact values of the critical field strengths or of the probability function will influence the numerical results but not in a fundamental way. Since the values used are within the region that would be expected from any separate consideration, we hold them to be uncritical.

Parameter A describing the desynchronization process is more critical. A back-of-the-envelope calculation looking at a simple Poisson equation that might pertain to the problem yields no usable result. Again, the value chosen must be taken as a prediction of the model to be justified either by more involved calculations or by experiments.

The strength of the model comes from two points: (*i*) It is physically sound and as simple as it can be to describe a complex phenomenon and (*ii*) It reproduces quantitatively a large number of experimental results, which could not be understood at all so far, with just one basic assumption and essentially only one truly fitted parameter.

The model makes many predictions (we do not discuss all of them here) that can be tested experimentally and thus is open to verification or falsification as it should be. In addition, it can be taken as a fundamental part of a more involved model that includes oscillation in the high-frequency regime. In this case the restriction of the model to cases where all the current produces oxide must be relaxed. It is necessary to include tunnel currents that flow through the oxide to accommodate, e.g., the infrequent galvanostatic experiments[13] where a constant current is impressed on the electrode and voltage oscillations (in a much more complex shape than current oscillations) are obtained. First attempts at looking at galvanostatic experiments were encouraging and will be published elsewhere.

Finally, our model is applicable to all electrodes, not only Si, where the basic process is an interplay of oxide formation and dissolution.

Christian-Albrechts-Universität Zu Kiel assisted in meeting the publication costs of this article.

Appendix

The calculation of the model is performed on two lattices $s_1(x, y)$ and $s_2(x, y)$, which store the coordinates of the upper and lower border, respectively, of the oxide layer for each point (x, y); e.g., the thickness $s(x, y)$ of the oxide layer is calculated by $s(x, y) = s_1(x, y) - s_2(x, y)$. The time evolution of both lattices is calculated by Monte Carlo simulation which refers to the fact that the dynamics of the occurrence and stop of an ionic breakthrough channel is defined by probability functions $W(E)$ and $R(E)$.

Knowing the location of each pore at every moment, the growth and dissolution of the oxide is defined by a set of differential equations. A discrete version of these differential equations allows calculation of $s_1(x, y, t + dt)$ and $s_2(x, y, t + dt)$, which is not a statistical process. The details of this calculation will be published elsewhere. Here we only stress some physical properties of the implemented differential equations

1. The pure chemical dissolution of the oxide-electrolyte surface, $s_1(x, y)$ is defined by the etching rate, α. Considering the increased area of a rough surface, the dissolution rate is enhanced, which leads to a smoothing of the surface roughness.

2. Through each open channel we assume a constant current $I_{ox,channel} = dQ_{ox,channel}/dt$. At each time step, dt, the semispherical inclusion around each channel tip is increased by $dV_{ox,channel} = \beta dQ_{ox,channel}$ which defines $ds_2(x, y)$. A current $I_{ox,channel} \approx 0.1$ fA builds up a sphere with about 5 nm radius within 10 s, which is in good agreement with our experimental results.

For the dynamics of the channels we define the functions

$$W(E) = \begin{cases} \exp - \left(\dfrac{E_{max} - E}{\Delta E_{max}}\right)^2 & \text{for } E \le E_{max} \\ 1 & \text{for } E > E_{max} \end{cases} \qquad [A\text{-}1]$$

$$R(E) = \begin{cases} \exp - \left(\dfrac{E - E_{min}}{\Delta E_{min}}\right)^2 & \text{for } E \ge E_{min} \\ 1 & \text{for } E < E_{min} \end{cases} \qquad [A\text{-}2]$$

The parameters E_{min} and E_{max} define upper and lower limits for the ionic breakthrough mechanism on an area ΔA in the nanometer scale within the time Δt. E_{min} and E_{max} are comparable to values for a perfect oxide, since the imperfection and inhomogeneity of the anodic oxide is described by the variances ΔE_{min} and ΔE_{max}. The variances ΔE_{min} and ΔE_{max} generate the randomness of the model and, in addition to the parameter ΔU_{an}, they define the strength of the desynchronization of the local oscillators. To obtain reasonable results for the Monte Carlo simulation we used $\Delta E/E \approx 0.15$ for E_{min} and E_{max}.

References

1. R. L. Smith and S. D. Collins, *J. Appl. Phys.*, **71**, R1 (1992).
2. H. Föll, *Appl. Phys. A.*, **53**, 8 (1991).
3. D. R. Turner, *J. Electrochem. Soc.*, **105**, 402 (1958).
4. H. Gerischer and M. Lübke, *Ber. Bunsen-Ges. Phys. Chem.*, **92**, 573 (1988).
5. M. Faraday, *Philos. Trans. R. Soc. London, Ser. A.*, **124**, 77 (1834).
6. V. Lehman and U. Gösele, *Appl. Phys. Lett.*, **58**, 856 (1991).
7. L. T. Canham, *Appl. Phys. Lett.*, **57**, 1046 (1990).
8. J. Stumper, R. Greef, and L. M. Peter, *J. Electroanal. Chem.*, **310**, 445 (1991).
9. F. Ozanam, J.-N. Chazalviel, A. Radi, and M. Etman, *J. Electrochem. Soc.*, **139**, 2491 (1992).
10. J.-N. Chazaviel and F. Ozanam, *J. Electrochem. Soc.*, **139**, 2501 (1992).
11. D. J. Blackwood, A. Borazio, R. Greef, L. M. Peter, and J. Stumper, *Electrochim. Acta*, **37**, 889 (1992).
12. H. J. Lewerenz and M. Aggour, *J. Electroanal. Chem.*, **351**, 159 (1993).
13. V. Lehmann, *J. Electrochem. Soc.*, **143**, 1313 (1996).
14. J. Carstensen, R. Prange, G. S. Popkirov, and H. Föll, *Appl. Phys. A.*, In press.
15. H. J. Lewerenz, *Chem. Soc. Rev.*, **26**, 239 (1997).
16. U. F. Franck, *Angew. Chem.*, **90**, 1 (1978).
17. J.-N. Chazalviel, F. Ozanam, M. Etman, F. Paolucci, L. M. Peter, and J. Stumper, *J. Electroanal. Chem.*, **327**, 343 (1992).
18. M. Aggour, M. Giersig, and H. J. Lewerenz, *J. Electroanal. Chem.*, **383**, 67 (1995).
19. O. Nast, S. Rauscher, H. Jungblut, and H. J. Lewerenz, *J. Electroanal. Chem.*, In Press.
20. J.-N. Chazalviel, *Electrochim. Acta*, **37**, 865 (1992).
21. Often observed, but not published except in V. Lehmann, PhD. Thesis, Erlangen (1988).
22. F. Ozanam, J.-N. Chazalviel, A. Radi, and M. Etman, *Ber. Bunsen-Ges. Phys. Chem.*, **95**, 98 (1991).
23. C. Sere, S. Barret, and R. Hérino, *J. Electrochem. Soc.*, **141**, 2049 (1994).
24. D. J. Dumin, *J. Electrochem. Soc.*, **142**, 1272 (1995).